Biochemical and Biophysical Research Communications 460 (2015) 362–367

Contents lists available at ScienceDirect

Biochemical and Biophysical Research Communications

journal homepage: www.elsevier.com/locate/ybbrc

# Chronopharmacodynamics and mechanisms of antitumor effect induced by erlotinib in xenograft-bearing nude mice

Pingping Lin [a, 1], Fengmei An [b, 1], Xia Xu [c], Liyan Zhao [c], Liang Liu [a], Ning Liu [a], Peipei Wang [d], Jiao Liu [e], Le Wang [a], Mingchun Li [c, *]

[a] Department of Pharmacology, Medical College of Qingdao University, Qingdao, China
[b] Hand Surgery Center of the Whole Army, No. 401 Hospital of Chinese People's Liberation Army, Qingdao, China
[c] Department of Pharmacy, No. 401 Hospital of Chinese People's Liberation Army, Qingdao, China
[d] Department of Clinical Pharmacy and Pharmaceutical Management, School of Pharmacy, Fudan University, Shanghai, China
[e] Department of Pharmacy, The Affiliated Hospital of Weifang Medical University, China

ARTICLE INFO

*Article history:*
Received 21 February 2015
Available online 17 March 2015

*Keywords:*
Chronopharmacology
Erlotinib
Circadian rhythms
NSCLC
HCC827

ABSTRACT

Receptor tyrosine kinases, mediators of a variety of critical cellular functions, contribute to tumor progression and metastasis. The epidermal growth factor receptor (EGFR), a member of the receptor tyrosine kinase family, is ubiquitously expressed on the surface of mammalian cells. Erlotinib hydrochloride (Tarceva) can inhibit the intracellular phosphorylation of tyrosine kinases. To investigate the influence of dosing time on the ability of erlotinib to inhibit tumor growth and the underlying molecular mechanisms via the PI3K/AKT and ERK/MAPK pathway, we established nude mice HCC827 tumor xenografts models. The tumor-bearing mice were housed 3–4 per cage under standardized light/dark cycle conditions (lights on at 07:00 h, off at 19:00 h) with food and water ad libitum. The mice were randomly divided into erlotinib treated groups and control groups, gavaged with erlotinib and vehicle respectively at 6 different time points for 21 days. To draw tumor growth curves, the tumor volume was measured every three days. After the mice were sacrificed, the tumor masses of each group were removed and weighed. The relative protein expression levels of p-EGFR, p-AKT and p-MAPK were assayed at 4 h after erlotinib or vehicle gavage by Western blot analysis. The antitumor effect of erlotinib presented diurnal rhythmicity. The growth of HCC827 xenograft was more potently inhibited by erlotinib in the early light phase than in the early dark phase ($p < 0.05$). The inhibitory effect of erlotinib on phosphorylation of EGFR, AKT and MAPK varied with its administration time. The results indicate that the antitumor effect of erlotinib is more potent when the drug was administered when the activities of EGFR and its downstream factors increased. Our findings may provide a clue to optimize the dosing schedule of erlotinib.



## 1. Introduction

Lung cancer, one of the most prevalent malignancies, is the leading cause of cancer-related death worldwide [1,2]. Of all the types of lung cancer, most cases are non-small-cell lung cancer (NSCLC), approximately accounting for 80–95% [3,4]. Although tumor recurrence and metastasis can largely be controlled by the traditional chemotherapy [5–7], it still causes severe side effects. Due to the better understanding of molecular mechanisms of tumorigenesis and the development in gene screening, small-molecule-targeted drugs have been designed to improve the treatment outcomes [8]. Erlotinib, a molecule-targeted drug, has been proved effective in the treatment of patients with advanced metastatic non-small-cell lung cancer, especially in patients with epidermal growth factor receptor (EGFR) mutation [9]. It is a tyrosine kinase inhibitor that suppresses intracellular phosphorylation of tyrosine kinase related to EGFR. EGFR is a crucial member of receptor tyrosine kinase family and is involved in plenty of cancer-related signal transduction pathways, such as proliferation, metastasis and angiogenesis [10]. Rat sarcoma/rapidly accelerated fibrosarcoma/mitogen-activated protein kinase (Ras/Raf/MAPK) and phosphatidylinositol-3-kinase/protein kinase B(PI3K/AKT) are two principal pathways of EGFR downstream, which can promote

* Corresponding author.
*E-mail address:* lmc401y@163.com (M. Li).
[1] These two authors contributed equally to this work and should be considered as co-first authors.

http://dx.doi.org/10.1016/j.bbrc.2015.03.039
0006-291X/

mitosis and prevent apoptosis [11]. Once the EGFR is autophosphorylated, the downstream signal is triggered.

Most of light-sensitive organisms possess physiological and behavioral rhythms which are consistent with 24-h day [12]. Circadian rhythms not only exist in normal physiological processes, but also in some pathophysiological courses, such as diabetes, cardiovascular disease, and autoimmune disease [12,13]. Recent understanding of the molecular control mechanisms of diurnal rhythms and subsequent signal pathways has revealed that the biological rhythmic variations might affect both the therapeutic effect and the side effects of the drugs [14,15]. It has been proved that treatment outcomes can be optimized by giving the drugs at appropriate time of a day by strengthening efficacy and reducing toxicities [16]. Although chronopharmacological strategy has been gradually used in clinical therapy and many patients benefit from it, many antitumor drugs are administered without instruction of optimal dosing-time.

The purpose of this study was to investigate the dosing time-dependent changes in the antitumor effects of erlotinib and the underlying mechanisms in tumor-bearing mice. It was expected that specific circadian time points can be selected to warrant further exploration of chronopharmacology of erlotinib in clinical trial.

## 2. Materials and methods

### 2.1. Media and reagents

RPMI 1640 (Hyclone, USA) was used as culture medium, supplemented with 10% fetal bovine serum (FBS) and 1% Penicillin–Streptomycin Solution. Erlotinib hydrochloride tablets (150 mg erlotinib/tablet) were provided by Roche Ltd. Because of its insolubility in water, erlotinib was made into suspension with the vehicles of Captisol [17,18] (sulfobutyl ether β-cyclodextrin, 6% solution in water), which was purchased from Medchemexpress LLC. Antibodies against phospho-EGFR, phospho-AKT, phospho-p44/42 MAPK (ERK1/2) and Glyceraldehyde-3-phosphate dehydrogenase (GAPDH) were purchased from Cell Signaling Technology (Boston, MA).

### 2.2. Animals and cells

Female BALB/c nude mice (4 weeks old) were purchased from Vital River Laboratory Animal Technology Co. Ltd. The mice were housed 4–5 per cage in light-controlled room (lights on at 07:00 h, off at 19:00 h) at a room temperature of 25 ± 3 °C and a humidity of 50 ± 10% with food and water available ad libitum. Before experiments, they were allowed to adapt to the standardized light/dark cycle for two weeks. All animal procedures were done in strict accordance with Animal Ethics Guidelines and approved by Ethic Committee of the No. 401 Hospital of Chinese People's Liberation Army.

HCC827, an EGFR-mutated cell line, was provided by Chinese Academy of Sciences, and maintained in RPMI 1640 medium supplemented with 10% FBS and 1% penicillin-streptomycin solution at 37 °C in a humidified atmosphere with 5% $CO_2$. After an adaptation period of two weeks, the mice were subcutaneously inoculated with a 200-μl volume of $1.0 \times 10^7$ viable HCC827 cells into the right flank.

### 2.3. Experimental design

To investigate the influence of dosing-time dependent changes on the antitumor effect induced by erlotinib, groups of 8 tumor-bearing nude mice were gavaged with a single daily dose (5 mg/kg) of erlotinib suspension (treatment groups) or vehicle (6% Captisol aqueous solution, model groups) at different circadian time (08:00, 12:00, 16:00, 20:00, 24:00 and morrow 04:00) for 21 days. After the final intragastric administration, tyrosine kinase activity of EGFR, AKT and MAPK of the non-drugged groups were detected by Western blot to explore whether 24-h oscillation existed in the phosphorylation of these proteins. To investigate the influence of dosing time on the ability of erlotinib to inhibit the phosphorylation of EGFR, AKT and MAPK, tumor-bearing mice were gavaged with erlotinib (5 mg/kg) suspension or vehicle at 08:00 or 20:00. At 4 h after administration, the phosphorylation state was detected by Western blotting.

### 2.4. Determination of antitumor effect

The influence of dosing-time on the antitumor effect of erlotinib was evaluated by the change of tumor volume and the tumor inhibition rate. The tumor volume was measured with caliper every three days and estimated according to the following formula: tumor volume ($mm^3$) = $a^2 \times b/2$, where $a$ is the shortest diameter and $b$ is the longest diameter. The tumor growth curves were drawn to describe the tendency of tumor volume change in each group. After the final administration, the mice were sacrificed and the xenografts were removed and weighed at the corresponding circadian time (08:00, 12:00, 16:00, 20:00, 24:00 and marrow 04:00). The tumor inhibition rate was calculated by the formula: tumor inhibition rate (%) = (average tumor weight of model group − average tumor weight of treatment group)/average tumor weight of model group × 100%.

### 2.5. Histopathological analysis

Three tumor masses were randomly collected from each group to do the histopathological analysis. They were fixed in 10% formalin overnight immediately after being removed. The fixed tumor masses were washed with flowing water for 8 h and cut into slices, and then dehydrated successively with 70%, 80%, 90% and pure ethanol. The slices were put into xylene solution for 40 min, dipped into molten paraffin and then made into paraffin blocks. After HE staining, the images were obtained under the optical microscope.

### 2.6. Western blot (WB) analysis

The frozen tumor masses were ground into powder by using liquid nitrogen. The total proteins were extracted in lysis buffer (50 mM Tris–HCl, pH 7.8, 150 mM NaCl, 5 mM EDTA, 0.5% Nonidet P-40, 2 mM PMSF, 1 mM $Na_3VO_4$) and quantified using the BCA method. The lysate samples were separated on SDS–PAGE (10%) and transferred to polyvinylidene fluoride (PVDF) membrane (Millipore, US). Subsequently, the PVDF membranes were incubated overnight at 4 °C with the following antibodies: GAPDH, anti-phospho-EGFR, anti-phospho-AKT and anti-phospho-p44/42 MAPK (1:1000; Cell Signaling Technology, MA). After incubation with horseradish peroxidase-linked anti-rabbit IgG (1:3000; Cell Signaling Technology, MA) at 37 °C for 1 h, bound proteins were made visible using immobilon Western chemiluminescent HRP substrate (Millipore, US) and detected by NIH image software. All the relative protein expression levels were calculated based on GAPDH protein as the loading control.

### 2.7. Statistical analysis

SPSS version 17.0 was used for all the analysis. The statistical significance among different groups was validated by one-way

ANOVA and Bonferroni test was used to compare the statistical significance of differences for multiple comparisons. A 5% level of probability was considered to be significant.

## 3. Results

### 3.1. Influence of erlotinib administration time on the antitumor effect

#### 3.1.1. Influence of administration time on tumor volume

Since there was no significant difference in the growth of tumors among the non-drugged groups, the mean value of the tumor volume from 6 model groups was regarded as the control. After the administration of erlotinib, the tumor growth of all the treatment groups was suppressed when compared with that of the model group (Fig. 1). Among all the treatment groups, tumor growth was more significantly suppressed and the tumors were smaller at the end of 21-day of administration in mice gavaged at 08:00 than at 20:00 ($p < 0.01$, respectively).

#### 3.1.2. Influence of administration time on tumor inhibition rate

Although the tumor weight of all the treatment groups was tremendously decreased when compared with the model group, the suppressive effect was more potent in the mice gavaged at 08:00 than at 20:00; namely, the tumor inhibition rate was the largest when erlotinib was given at 08:00 ($p < 0.01$, Table 1).

#### 3.1.3. Influence of administration time on histopathology

We also detected the influence of erlotinib dosing-time on histopathology. The 7 photographs in Fig. 2 respectively represent the images of sections of tumor tissues from 6 erlotinib treated groups gavaged at different circadian times and from the model group. Poorly differentiated and tightly arranged tumor cells were observed in the mice of the model group without obvious necrosis of tumor cells. Large areas of cystic degeneration and inflammatory infiltration can be easily spotted in the tumor tissue of mice given erlotinib at 08:00, 12:00 and 04:00, and the tumor cells arranged irregularly with necrosis and minimal bleeding. Although inflammatory ooze, necrosis and cystic degeneration can also be observed in the mice gavaged with erlotinib at 16:00, 20:00 and 24:00, the levels were much lower than that of the mice gavaged at 08:00, 12:00 and 04:00.

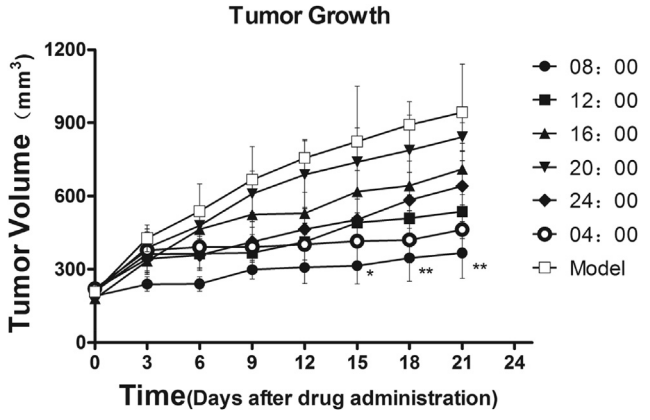


**Fig. 1.** Influence of administration time on the ability of erlotinib to inhibit the tumor growth. Erlotinib (5 mg/kg, bid.) (08:00, 12:00, 16:00, 20:00, 24:00, 04:00) or vehicle was gavaged every day for 21 days. Each value is the mean with S.E. of 8 mice. $^{*}p < 0.05$, $^{**}p < 0.01$ when compared with the model group using Bonferroni-test.

**Table 1**
Comparison of transplanted tumor weight and inhibition rate in each group ($x \pm s$, $n = 8$).

| Group | Tumor weight (g) | Tumor inhibition rate (%) |
|---|---|---|
| Model | 0.74 ± 0.26 | – |
| 08:00 | 0.30 ± 0.17** | 59.24 |
| 12:00 | 0.48 ± 0.34* | 34.50 |
| 16:00 | 0.61 ± 0.35 | 17.10 |
| 20:00 | 0.70 ± 0.36 | 5.14 |
| 24:00 | 0.59 ± 0.32 | 19.81 |
| 04:00 | 0.39 ± 0.29* | 47.72 |

$^{*}p < 0.05$, $^{**}p < 0.01$ when compared with the model group.

### 3.2. Influence of administration time on the ability of erlotinib to inhibit the phosphorylation of EGFR

Erlotinib exerts its anti-tumor effect by inhibiting the intracellular phosphorylation of tyrosine kinase which is related to EGFR. We investigated whether the administration time can affect the ability of erlotinib to inhibit the phosphorylation of EGFR. Under non-drugged state, the phosphorylation of EGFR showed obvious oscillation ($p < 0.05$, Fig. 3A). From the late dark phase (24:00 and 04:00) to the early light phase (08:00 and 12:00), the relative expression level of p-EGFR was higher than the late light phase (16:00) and the early dark phase (20:00). Then we detected the expression of p-EGFR in mice gavaged with erlotinib at 08:00 and 20:00. Since erlotinib concentration in tumor mass can reach the peak about 4 h after administration [19], the expression of p-EGFR was assessed at 4 h after erlotinib gavage. As we can see in Fig. 3B, the phosphorylation of EGFR was more significantly inhibited by erlotinib than vehicle at 08:00 ($p < 0.01$), while there was no significant difference in the expression of p-EGFR between the model group and the treatment group at 20:00.

### 3.3. Influence of administration time on the ability of erlotinib to suppress the phosphorylation of AKT and p44/42 MAPK

Ras/Raf/MAPK and PI3K/AKT are two chief downstream signal pathways of EGFR [20]. Once the EGFR is autophosphorylated, the downstream signal will be triggered. We investigated whether the administration time had the same effect on the phosphorylation of AKT and p44/42 MAPK. The study procedure was the same as that of investigating p-EGFR. Under non-drugged state, the expressions of p-AKT and p-p44/42 MAPK protein showed obvious 24-h oscillation, which was similar to the phosphorylation of EGFR (Fig. 4A and C). The expressions of p-AKT and p-p44/42 MAPK protein at 4 h after erlotinib gavaging were significantly lower than those of their corresponding vehicle groups gavaged at 08:00 ($p < 0.01$, Fig. 4B and D). There was no significant difference in the expressions of p-AKT or p-p44/42 MAPK proteins between the model group and the treatment group at 20:00.

## 4. Discussion

This study has demonstrated that the antitumor effect of erlotinib varied with its administration time in HCC827 implanted nude mice. The ability of erlotinib to inhibit the tumor growth was more pronounced when it was given at the early light phase than at the early dark phase. The results correspond with previous chronopharmacological studies on the antitumor effect of interferon-β, TNP-470 and imatinib [21–23].

Diurnal rhythmic oscillation in biological functions, such as signal transduction and receptor sensitivity, is thought to be related with the efficacy and toxicity of drugs. Erlotinib, acting as ATP

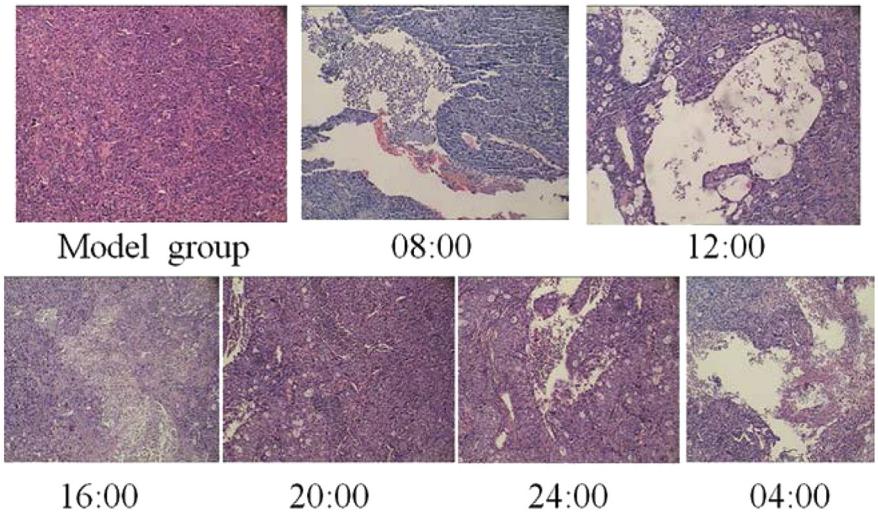


**Fig. 2.** Microscopic images of pathological sections from model group and erlotinib-gavaged groups after 21 days of administration (HE staining, original magnification ×100). Model group: Pathological section from the mice gavaged with vehicle. The tumor cells arranged tightly without obvious necrosis and cystic degeneration. Group 8:00, 12:00 and 04:00: Pathological sections from the mice gavaged with erlotinib at 08:00, 12:00 and 04:00, respectively. Large areas of cystic degeneration and inflammatory infiltration can be easily observed. Necrosis and minimal bleeding can also be found. Group 16:00, 20:00, 24:00: Pathological sections from the mice gavaged with erlotinib at 16:00, 20:00 and 24:00: Small areas of inflammatory ooze, necrosis and cystic degeneration can be observed with the irregular arrangement of tumor cells.

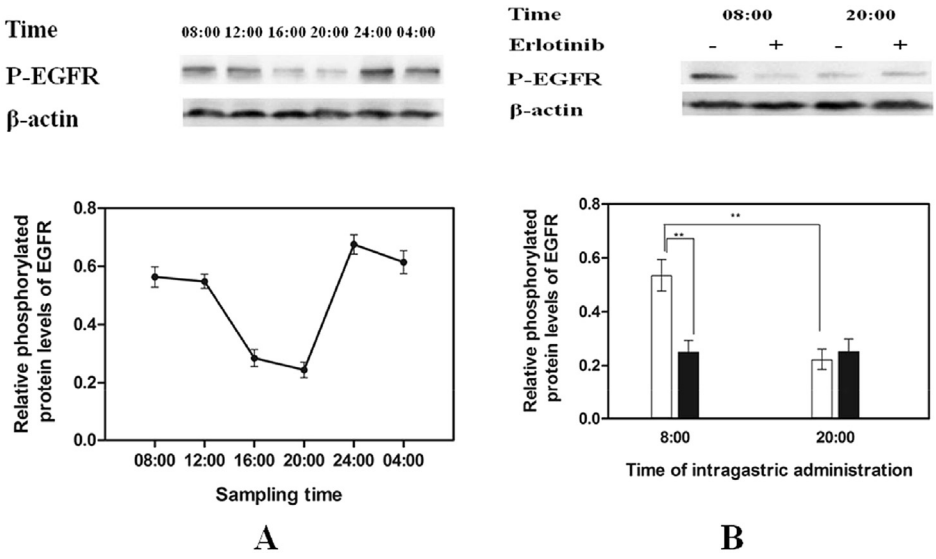


**Fig. 3.** Tyrosine kinase activity of EGFR under non-drugged state (A) and the influence of administration time on the ability of erlotinib to inhibit the phosphorylation of EGFR (B). The protein level is normalized by β-actin. Each value is the mean with S.E. of 5 or 6 mice. The expression of p-EGFR presents 24-h variations ($p < 0.05$, ANOVA) under non-drugged state. The mice were given a single intragastric administration of erlotinib (■) or vehicle (□) at 08:00 and 20:00, respectively. $^{*}p < 0.05$, $^{**}p < 0.01$ when compared between groups using Bonferroni-test.

mimetic agents, inhibits the binding of ATP to the pocket domain and consequently restrains the phosphorylation of EGFR and its downstream pathways [24]. Namely, EGFR is the target of erlotinib to exert its antitumor effect. For a higher sensitivity to erlotinib in mutated-EGFR tumors [25,26], we chose EGFR mutation cell line HCC827 to establish the xenograft mouse model. Ras/Raf/MAPK and PI3K/AKT are two principal pathways of EGFR downstream, which contribute to cell survival (apoptosis) and cell growth. Although different mutation types of EGFR are different in activating EGFR downstream signaling pathways [27–30], the p-p44/42 MAPK is highly susceptible to the inhibitory effect of erlotinib just as p-AKT in HCC827 [31]. Therefore, we detected the underlying mechanisms of dosing-time-dependent change from the activation of EGFR and its downstream pathways.

Under non-drugged states, the phosphorylation of EGFR showed significant rhythmic variation, which is similar to the findings of Lauriola et al. [32]. We also found that the anti-EGFR drug, given during the resting phase instead of the active phase, showed more potent anti-tumor efficacy in animals. EGFR, which is expressed in the core circadian pacemaker and transcription-factors, is implicated in circadian function and responsible for the circadian phase-dependent EGFR responses [33]. Therefore, one possible mechanism accounting for the oscillation in p-EGFR expression is that the core circadian clock influences EGFR gene and then affects the protein expression level. Several EGF family ligands, which are bound to EGFR, can mediate the dimerization of EGFR and ensue autophosphorylation [34]. Thereby, it is also probable that the binding amount of these EGF family ligands to EGFR varies with

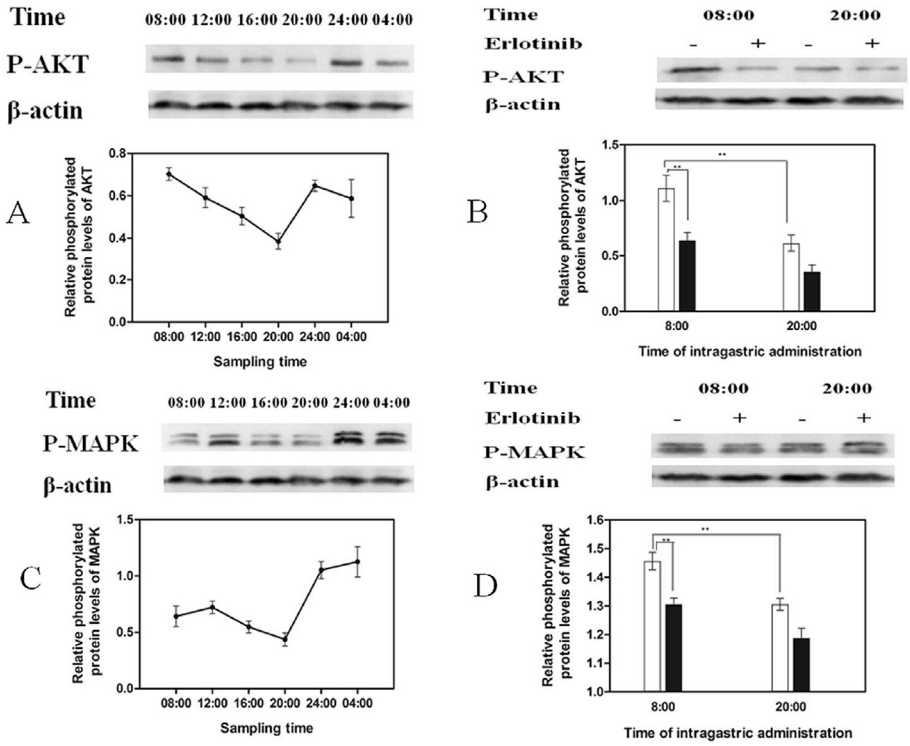


**Fig. 4.** Tyrosine kinase activity of AKT and p44/42 MAPK under non-drugged state (A and C) and the influence of administration time on the ability of erlotinib to inhibit the phosphorylation of AKT and p44/42 MAPK (B and D). The protein level is normalized by β-actin. Each value is the mean with S.E. of 5 or 6 mice. The expression of p-AKT and p-p44/42 MAPK presents 24-h variations ($p < 0.05$, ANOVA) under non-drugged state. The mice were given a single intragastric administration of erlotinib (■) or vehicle (□) at 08:00 and 20:00, respectively. $^{*}p < 0.05$, $^{**}p < 0.01$ when compared between groups using Bonferroni-test.

different circadian times. The phosphorylation of EGFR was notably inhibited by erlotinib gavaged at 08:00 than at 20:00, which implies that there are dosing-time dependent changes in the suppression effect of erlotinib, and it seems to be induced by the 24-h oscillation in the expression of p-EGFR. EGFR is a member of receptor tyrosine kinase family, whose gene is recognized as oncogene [35]. EGFR are considered to be related with plenty of tumor growth processes. As a result, the dosing-time dependent changes induced by erlotinib on the expression of p-EGFR may contribute to the different anti-tumor effects at different times. As it is well known, Ras/Raf/MAPK and PI3K/AKT are two crucial signal pathways involved in EGFR signaling cascade and both of them are closely related to cell growth and apoptosis. The inhibitory effect of erlotinib on the tyrosine kinase activity of both AKT and p44/42 MAPK shows the same tendency as that of EGFR. Overall, the dosing-time dependent changes on the inhibitory effect of EGFR-ERK/MAPK and EGFR-PI3K/AKT signal pathways induced by erlotinib seems to be involved in the mechanism of the 24-h variation in the antitumor effect of erlotinib.

This study demonstrates a potential mechanism underlying the 24-h oscillation in antitumor effect of erlotinib in HCC827 xenograft nude mice. Furthermore, diurnal rhythmic changes in the receptor tyrosine kinase activities of EGFR and its downstream signal pathways seem to influence the dosing-time dependent changes of antitumor effect induced by erlotinib. A rational chronotherapeutic strategy of erlotinib could be expected by choosing the most appropriate administration time. Our results may provide a clue for reasonable usage of erlotinib in its further clinical chronopharmacological research. In the future, we will perform further studies on the chronopharmacokinetics in the mice model and clinical chronopharmacological administration strategy of erlotinib.

## Conflict of interest

None.

## Acknowledgments

We would like to thank the Department of Pathology of the No 401 Hospital of the PLA for providing the valuable help. We would like to thank Prof. Linxiang Guo for providing language help and Prof. Zhaori for critical reading of the manuscript.

## Transparency document

The Transparency Document associated with this article can be found in the online version at http://dx.doi.org/10.1016/j.bbrc.2015.03.039.

## References

[1] Jacques Ferlay, Hai-Rim Shin, Freddie Bray, et al., Estimates of worldwide burden of cancer in 2008: GLOBOCAN 2008, Int. J. Cancer 27 (2010) 2893–2917.
[2] Ahmedin Jemal, Rebecca Siegel, Elizabeth Ward, et al., Cancer statistics, 2008, CA Cancer J. Clin. 58 (2008) 71–96.
[3] L. Crino, W. Weder, J. van Meerbeeck, et al., Early stage and locally advanced (non-metastatic) non-small-cell lung cancer: ESMO clinical practice guidelines for diagnosis, treatment and follow-up, Ann. Oncol. 21 (Suppl. 5) (2010) 103–105.
[4] W. Smith, F.R. Khuri, The care of the lung cancer patient in the 21st century: a new age, Semin. Oncol. 31 (2 Suppl. 4) (2004) 11–15.
[5] J.H. Schiller, D. Harrington, C.P. Belani, et al., Comparison of four chemotherapy regimens for advanced non-small-cell lung cancer, N. Engl. J. Med. 346 (2002) 92–98.
[6] F. Fossella, J.R. Pereira, J. von Pawel, et al., Randomized, multinational, phase III study of docetaxel plus platinum combinations versus vinorelbine plus

cisplatin for advanced non-small-cell lung cancer: the TAX326 study group, J. Clin. Oncol. 21 (2003) 3016–3024.
[7] Julian R. Molina, Ping Yang, Stephen D. Cassivi, et al., Non-small cell lung cancer: epidemiology, risk factors, treatment, and survivorship, Mayo Clin. Proc. 83 (2008) 584–594.
[8] Yongjun Guo, Jie Ma, Xiaodong Lyu, et al., Non-small cell lung cancer with EML4-ALK translocation in Chinese male never-smokers is characterized with early-onset, BMC Cancer 14 (2014) 834.
[9] Barbara Melosky, Review of EGFR TKIs in metastatic NSCLC, including ongoing trials, Front. Oncol. 4 (2014) 244.
[10] M. Steins, M. Thomas, M. Geißler, Erlotinib recent results, Cancer Res. 201 (2014) 109–123.
[11] John R. Goffin, Kevin Zbuk, Epidermal growth factor receptor: pathway, therapies, and pipeline, Clin. Ther. 35 (2013) 1282–1303.
[12] Kristine Griffett, Thomas P. Burris, The mammalian clock and chronopharmacology, Bioorg. Med. Chem. Lett. 23 (2013) 1929–1934.
[13] J. Sprouse, Pharmacological modulation of circadian rhythms: a new drug target in psychotherapeutics, Expert Opin. Ther. Targets 8 (2004) 25–38.
[14] Francis Lévi, Chronotherapeutics: the relevance of timing in cancer therapy, Cancer Causes Control 17 (2006) 611–621.
[15] Marie-Christine Mormont, Francis Levi, Cancer chronotherapy: principles, applications, and perspectives, Cancer 97 (2003) 155–169.
[16] Michael H. Smolensky, Nicholas A. Peppas, Chronobiology, drug delivery, and chronotherapeutics, Adv. Drug Deliv. Rev. 59 (2007) 828–851.
[17] Thomas Friess, Werner Scheuer, Max Hasmann, Combination treatment with erlotinib and pertuzumab against human tumor xenografts is superior to monotherapy, Clin. Cancer Res. 11 (2005) 5300–5309.
[18] L.K. Zerbe, L.D. Dwyer-Nield, J.M. Fritz, et al., Inhibition by erlotinib of primary lung adenocarcinoma at an early stage in male mice, Cancer Chemother. Pharmacol. 62 (2008) 605–620.
[19] Solange Peters, Stefan Zimmermann, Alex A. Adjei, Oral epidermal growth factor receptor tyrosine kinase inhibitors for the treatment of non-small cell lung cancer: comparative pharmacokinetics and drug–drug interactions, Cancer Treat. Rev. 40 (2014) 917–926.
[20] H. Kitano, J.Y. Chung, K. Ylaya, et al., Profiling of phospho-AKT, phospho-mTOR, phospho-MAPK and EGFR in non-small cell lung cancer, J. Histochem. Cytochem. 62 (2014) 335–346.
[21] T. Hiroshi, H.O. Shigehiro, Y. Tomoko, et al., Chronopharmacology of anti-tumor effect induced by interferon-β in tumor-bearing mice, J. Pharmacol. Exp. Ther. 294 (2000) 746–752.
[22] K. Satoru, N. Hiroo, K. Yukako, et al., Optimizing the dosing schedule of TNP-470 [O-(chloroacetylcarbamoyl) fumagillol] enhances its antitumor and antiangiogenic efficacies, J. Pharmacol. Exp. Ther. 304 (2003) 669–674.
[23] N. Hiroo, T. Takako, N. Mariko, et al., Basis for dosing time-dependent change in the anti-tumor effect of imtinib in mice, Biochem. Pharmacol. 72 (2006) 1237–1245.
[24] Alba A. Brandes, Enrico Franceschi, Alicia Tosoni, et al., Epidermal growth factor receptor inhibitors in neuro-oncology: hopes and disappointments, Clin. Cancer Res. 14 (2008) 957–960.
[25] Niels Reinmuth, Michael Meister, Thomas Muley, et al., Molecular determinants of response to RTK-targeting agents in nonsmall cell lung cancer, Int. J. Cancer 119 (2006) 727–734.
[26] Hongbin Ji, Danan Li, Liang Chen, et al., The impact of human EGFR kinase domain mutations on lung tumorigenesis and in vivo sensitivity to EGFR-targeted therapies, Cancer Cell 9 (2006) 485–495.
[27] X. Sui, N. Kong, M. Zhu, et al., Cotargeting EGFR and autophagy signaling: a novel therapeutic strategy for non-small-cell lung cancer, Mol. Clin. Oncol. 2 (2014) 8–12.
[28] R. Sodella, D.W. Bell, D.A. Haber, et al., Gefitinib-sensitizing EGFR mutations in lung cancer activate anti-apoptotic pathways, Science 305 (2004) 1163–1167.
[29] J.G. Paez, P.A. Janne, J.C. Lee, et al., EGFR mutations in lung cancer: correlation with clinical response to gefitinib therapy, Science 304 (2004) 1497–1500.
[30] Sean Tracy, Toru Mukohara, Mark Hansen, et al., Gefitinib induces apoptosis in the EGFRL858R non-small-cell lung cancer cell line H3255, Cancer Res. 64 (2004) 7241–7244.
[31] Zhenfeng Zhang, Susumu Kobayashi, Alain C. Borczuk, Dual specificity phosphatase 6 (DUSP6) is an ETS-regulated negative feedback mediator of oncogenic ERK signaling in lung cancer cells, Carcinogenesis 31 (2010) 577–586.
[32] Mattia Lauriola, Yehoshua Enuka, Amit Zeisel, et al., Diurnal suppression of EGFR signalling by glucocorticoids and implications for tumour progression and treatment, Nat. Commun. 5 (2014) 5073.
[33] Daniel E. Zak, Haiping Hao, Rajanikanth Vadigepalli, et al., Systems analysis of circadian time-dependent neuronal epidermal growth factor receptor signaling, Genome Biol. 7 (2006) R48.
[34] Wymke Ockenga, Sina Kühne, Simone Bocksberger, et al., Epidermal growth factor receptor transactivation is required for mitogen-activated protein kinase activation by muscarinic acetylcholine receptors in HaCaT keratinocytes, Int. J. Mol. Sci. 15 (2014) 21433–21454.
[35] M. Berg, K. Soreide, EGFR and downstream genetic alterations in KRAS/BRAF and PI3K/AKT pathways in colorectal cancer: implications for targeted therapy, Discov. Med. 14 (2012) 207–214.